The Glucocorticoid Receptor Is a Key Player for Prostate Cancer Cell Survival and a Target for Improved Antiandrogen Therapy

Martin Puhr[1], Julia Hoefer[1], Andrea Eigentler[1], Christian Ploner[2], Florian Handle[1], Georg Schaefer[3], Jan Kroon[4,5], Angela Leo[1], Isabel Heidegger[1], Iris Eder[1], Zoran Culig[1], Gabri Van der Pluijm[6], and Helmut Klocker[1]

Abstract

Purpose: The major obstacle in the management of advanced prostate cancer is the occurrence of resistance to endocrine therapy. Although the androgen receptor (AR) has been linked to therapy failure, the underlying escape mechanisms have not been fully clarified. Being closely related to the AR, the glucocorticoid receptor (GR) has been suggested to play a role in enzalutamide and docetaxel resistance. Given that glucocorticoids are frequently applied to prostate cancer patients, it is essential to unravel the exact role of the GR in prostate cancer progression.

Experimental Design: Assessment of GR expression and functional significance in tissues from 177 prostate cancer patients, including 14 lymph node metastases, as well as in several human prostate cancer models, including androgen-dependent, androgen-independent, and long-term antiandrogen-treated cell lines.

Results: Although GR expression is reduced in primary prostate cancer tissue, it is restored in metastatic lesions. Relapse patients with high GR experience shortened progression-free survival. GR is significantly increased upon long-term abiraterone or enzalutamide treatment in the majority of preclinical models, thus identifying GR upregulation as an underlying mechanism for cells to bypass AR blockade. Importantly, GR inhibition by RNAi or chemical blockade results in impaired proliferation and 3D-spheroid formation in all tested cell lines.

Conclusions: GR upregulation seems to be a common mechanism during antiandrogen treatment and supports the notion that targeting the GR pathway combined with antiandrogen medication may further improve prostate cancer therapy. *Clin Cancer Res; 24(4); 927–38. ©2017 AACR.*

Introduction

The development of novel drugs that target androgen receptor (AR) signaling, such as abiraterone (1, 2) and enzalutamide (3, 4), has expanded the limited therapeutic options for treatment of prostate cancer. Both drugs are administered to patients with metastatic castration-resistant prostate cancer (mCRPC) before or after chemotherapy, resulting in prolonged progression-free and overall survival. However, therapy of such tumor stages remains palliative and is often limited due to the rapid development of drug resistance (5–7). In this context, the AR is known as a prime suspect; however, AR modifications, including AR gene amplification, upregulation of AR variants (8), and AR point mutations (9), can only partially explain drug insensitivity. This underscores the importance of identifying new molecular events associated with drug resistance to overcome therapy failure.

Being closely related to the AR, the glucocorticoid receptor (GR) is hypothesized to participate in therapy resistance. In the absence of glucocorticoids (e.g., cortisol, prednisolone, dexamethasone), the GR is sequestered in the cytoplasm by chaperone proteins. Ligand binding leads to rapid GR dimerization and nuclear translocation, which subsequently influences target gene expression (10, 11). Glucocorticoids are currently being used in the management of several tumor types, including mCRPC, as they suppress the secretion of adrenocorticotrophic hormone, thus resulting in reduced expression of adrenal androgens and consequently in a decline in PSA and circulating tumor cells (12). In addition, glucocorticoids exert anti-inflammatory as well as anti-emetic effects and are therefore frequently given to patients in combination with docetaxel, cabazitaxel (13–15), and abiraterone (16, 17) to suppress severe therapy-related adverse effects. However, their independent impact on survival is unclear, and unfavorable effects, such as osteoporosis and immunosuppression, complicate long-term use (12). Recently, elevated GR expression has been associated with resistance to enzalutamide therapy (18, 19). In particular, enhanced GR expression was observed in enzalutamide-resistant tumors *in vivo* and in tumor biopsies from enzalutamide-treated prostate cancer patients (18). These findings might be explained by the fact that AR can directly repress GR

[1]Department of Urology, Medical University of Innsbruck, Innsbruck, Austria. [2]Department of Plastic, Reconstructive and Aesthetic Surgery Innsbruck, Medical University of Innsbruck, Innsbruck, Austria. [3]Department of Pathology, Medical University of Innsbruck, Innsbruck, Austria. [4]Department of Medicine, Division of Endocrinology, Leiden University Medical Center, Leiden, the Netherlands. [5]Einthoven Laboratory of Experimental Vascular Medicine, Leiden University Medical Center, Leiden, the Netherlands. [6]Department of Urology, Leiden University Medical Center, Leiden, the Netherlands.

AACR 927

Translational Relevance

Management of advanced prostate cancer is restricted by the inevitable occurrence of endocrine therapy resistance, which results in rapid disease progression. This study identifies the glucocorticoid receptor (GR) as a crucial survival factor for prostate cancer cells and its upregulation as a frequent mechanism to bypass androgen receptor blockade by abiraterone or enzalutamide. As glucocorticoids are currently used in the management of metastatic castration-resistant prostate cancer in combination with docetaxel, cabazitaxel, and abiraterone, it has to be assumed that this therapeutic strategy might further promote selection of GR[high] drug-insensitive prostate cancer cells and accelerate disease progression. Therefore, the usefulness of glucocorticoids in such a therapeutic setting needs to be carefully reevaluated. Moreover, preclinical *in vitro* data combined with GR expression profiles in prostate cancer patient material presented herein provide a strong rationale for the clinical use of GR antagonists in combination with antiandrogens to further optimize treatment of endocrine therapy–naïve and resistant prostate cancer.

expression in prostate cancer via a negative androgen response element (ARE) in the GR promoter (20). Therefore, it was proposed that GR can functionally replace the AR, when AR signaling is blocked. Consistently, it has been shown that both receptors not only exhibit a significant overlap in their transcriptome (18), but also share several interacting proteins (21). In line with these observations, stimulation of GR activity could rescue cells from enzalutamide-induced cell death (18). In addition to modulating the efficacy of antiandrogens, dexamethasone administration undermined the antitumor effects of paclitaxel *in vitro* and *in vivo*, thus giving rise to chemotherapy resistance (22). In concordance with these results, we previously observed increased GR expression in tissue of patients after neoadjuvant docetaxel treatment as well as in docetaxel-resistant cell lines. Moreover, drug resistance could be reversed via administration of the GR inhibitor RU-486 (mifepristone), suggesting a beneficial effect of GR antagonist administration during standard chemotherapy treatment (23).

To elucidate the putative beneficial effects of GR targeting, this study addressed whether GR inhibition can be exploited for treatment of endocrine therapy–naïve and resistant prostate cancer.

Materials and Methods

Cell culture and chemicals

PC3, DU145, LNCaP, CWR22Rv1, VCaP, MDA-MB231, MCF7, T47D, and BT-20 cells were obtained from the ATCC. LAPC4 were a gift from Dr. A. Cato (University of Karlsruhe, Karlsruhe, Germany). BPH-1 and DUCaP cells were a gift from Dr. J Schalken (Radboud University, Nijmegen, the Netherlands). LNCaPabl cells were established after long-term cultivation of LNCaP cells in steroid-free medium and were cultured as described previously (24). RWPE-1 and EP156T cells were cultured as described previously (25, 26). Cancer-associated fibroblasts and normal-associated fibroblast cells have been generated and cultured as described in ref. 27. PC3, DU145, LNCaP, CWR22Rv1,

LAPC4, T47D and MDA-MB231, BPH1, and DUCaP were cultured in RPMI1640 supplemented with 10% FCS (Biowest), 1% penicillin/streptomycin (Szabo Scandic), and 1× GlutaMAX (Thermo Fisher Scientific). LAPC4 were further supplemented with 1 nmol/L DHT. VCaP were grown in DMEM supplemented with 10% FCS, 1× GlutaMAX, and 1.75 g D-glucose. MCF7 and BT-20 were grown in EMEM medium supplemented with 10% FCS (Biowest), 1× GlutaMAX (Thermo Fisher Scientific) and 1% penicillin/streptomycin (Szabo Scandic). For MCF7, 1% nonessential amino acids (Sczabo Scandic) and 0.01 mg/mL insulin have been added. Dexamethasone (1 μmol/L; Selleck Chemicals) was used to activate GR signaling in specific experiments. Before project start, identity of used cell lines was confirmed by short tandem repeat analysis. All cell lines have been used for a maximum of 20 to 30 passages.

Generation of long-term abiraterone- and enzalutamide-treated cell lines

LNCaPabl, DUCaP, and LAPC4 cells were cultured in the presence of increasing doses of abiraterone (Hycultec) or vehicle (EtOH). Drug treatment was started using 0.2 μmol/L of abiraterone. Drug-containing medium was changed every third day. Abiraterone concentration was increased when cells started to regrow in the presence of the drug at a growth rate similar to that of control cells until a final concentration of 4 μmol/L for DUCaP, 8 μmol/L LAPC4, and 8 μmol/L for LNCaPabl cells. The established cell sublines were named DUCaP-Ctrl/-Abi, LAPC4-Ctrl/-Abi, and LNCaPabl-Ctrl/-Abi. Generation of control- or long-term enzalutamide-treated LNCaPabl, DUCaP, and LAPC4 (termed LNCaPabl-Ctrl/-Enza, DUCaP-Ctrl/-Enza, LAPC4-Ctrl/-Enza) has been described in a previous study (8). Long-term enzalutamide-treated LNCaP (LNCaP-Enza) cells were generated by continuous exposure to 1 μmol/L enzalutamide until a sustained increase in proliferation was observed. Subsequently, drug concentration was increased to 5 μmol/L. Identity of the used cell lines was confirmed after cell subline establishment by short tandem repeat analysis. All cell lines have been used for a maximum of 20 to 30 passages. Representative brightfield images of all cells were taken using an Olympus CK2 microscope (Olympus) equipped with a ProgRes CT3 Camera (JENOPTIK) and the ProgRes CapturePro Software 2.9.0.1 (JENOPTIK).

Generation of doxycycline-inducible lentiviral vectors and plasmid construction

Complementary shRNA oligonucleotides directed against the human GR (5′-GATCCCCCCACAGGCTTCAGGTATCTTATTT-CAAGAGAATAAGATACCTGAAGCCTGTGTTTTTGGAAA-3′ for shGR-1 and 5′-GATCCCCGGATGTCATTATGGAGTCTTATT CAA-GAGATAAGACTCCATAATGACATCCTTTTTGGAAA-3′ for shGR-2 (targeting sequences are underlined) containing BamHI and HindIII sticky ends were used and synthesized by the company Microsynth. Oligonucleotides were phosphorylated, annealed, and cloned into the BglII-HindIII sites of pENTR-THT (28). The sequence-verified THT-shRNA cassettes were recombined into the GATEWAY-based lentiviral tetracycline-regulated conditional RNAi vector pGLTR-X as described in detail (28). GR knockdown in the established shGR cell lines was achieved by adding 1 μg/mL doxycycline to the media for 6 days. Any unspecific side effects of doxycycline up to 4 μg/mL could be already excluded in a previous publication (29).

Generation of lentiviral particles and cell infection

Lentiviral transduction of target cells was performed as described previously (28). In brief, confluent HEK293T cells were transfected with 1.5 µg lentiviral vector and 0.9 µg of each packaging plasmid [psPAX2, pMD-G VSV-G, both vectors were kindly provided by D. Trono (EPFL, Lausanne, Switzerland)] by CaPO$_4$-based transfection. Virus-containing cell supernatant was harvested after 48 and 72 hours, filtered, and added to the target cells in presence of 1 µg/mL polybrene. Seventy-two hours after infection, cells were selected with 2.5 µg/mL puromycin (Sigma) for 2 weeks to obtain a clean pool of transduced cells.

Patient material and IHC

Tissue samples were selected from the Innsbruck prostate cancer biobank. The use of archived material was approved by the Ethics Committee of the Medical University of Innsbruck (study no. AM 3174 including amendment 2). Written consent was obtained from all patients and documented in the database of the University Hospital Innsbruck (Innsbruck, Austria) in agreement with statutory provisions. Tissue microarrays (TMA) containing benign and primary cancer tissue cores from 177 prostate cancer patients who underwent open retropubic or robotic assisted (Da Vinci) radical prostatectomy (RPE) at the University Hospital Innsbruck and cores of lymph node metastases from 14 prostate cancer patients (taken at the time of RPE) were employed to evaluate GR expression. The matched benign samples were excised from histologically confirmed nonmalignant regions of RPE specimens. A summary of patient characteristics and descriptive histology at the time of RPE is provided within Supplementary Table S1. GR IHC was performed on a Discovery - XT staining device (Ventana). The following antibody was used: anti-GR rabbit mAb (D6H2L; 1:200; Cell Signaling Technology). Specificity of the used GR antibody was confirmed by Western blot analysis and IHC staining of DU145 cells after transient transfection with either 40 nmol/L of on-target-plus siGR pool (L-003424-00-0005, Dharmacon Inc.) or GR expression vector pCMV6-XL5-GR (Origene Technologies Inc.) for 3 days. For IHC, cells were harvested and resuspended in 450 µL citrate plasma and 11.3 µL 1 mol/L calcium chloride in a 15-mL vial. Thrombin 120 NIH-U/mL (45 µL; Promega) was added until the cell suspension coagulated. The coagulate was transferred in a biopsy histosette, formalin fixed, and paraffin embedded. TMAs were evaluated using the following modified "quick - score" protocol: staining intensity was scored 0 to 3 (0 = absent, 1 = weak, 2 = intermediate, 3 = strong). The percentage of positively stained cells was scored 0 to 4 (0 = absent, 1 = <10%, 2 = <50%, 3 = <75%, 4 = >75%). Both scores were multiplied to obtain an immunoreactivity score (IRS), ranging from 0 to 12. For survival analysis, samples from patients with confirmed biochemical relapse within 10 years from RPE [$n = 24$; relapse = rising PSA levels (>0.2 ng/mL) in 2 subsequent measurements] at a known time point have been included. For that, patients have been divided into intermediate/high GR (IRS $\geq$ 3.5) or low GR (IRS $\leq$ 3.5) groups, based on GR immunoreactivity scores in malignant tissue specimens.

RNA isolation from prostate tissue

Forty representative RPE prostate cancer patients were selected from the tissue database of the Department of Urology. The use of archived material was approved by the Ethics Committee of the Medical University of Innsbruck (study no. AM 3174 including amendment 2). Frozen prostate tissue sections from selected patients were macrodissected with benign and malignant samples taken for each patient. Total RNA was isolated with Direct-zol RNA MiniPrep (Zymo Research) Kit according to the manufacturer's protocol. The amount, integrity, and quality of isolated RNA were determined by assessment of the RNA integrity number (RIN) on an Agilent 2100 bioanalyzer (Agilent Technologies) and 260/280 as well as 230/260 optical density (OD) ratios on a NanoDrop2000 (Thermo Fisher Scientific). Only samples with a minimum measured RIN of 7 and appropriate OD ratios were considered for further evaluation.

RNA isolation from cell lines

Total RNA from cell lines was isolated with the RNeasy Mini Kit (Qiagen) according to the manufacturer's instructions. Quality and amount of isolated RNA were determined on a Nano-Drop2000 system (Thermo Fisher Scientific).

cDNA synthesis and qRT-PCR

cDNA was synthesized using the iScript cDNA Synthesis Kit (Bio-Rad, Vienna), and qRT-PCR was performed on an ABI PRISM 7500-FAST qRT-PCR system (Thermo Fisher Scientific). Either *TBP* or *HPRT1* (cell lines) or the mean of TBP and HPRT1 (tissue samples) were used as housekeeping genes for normalization. Primer and probe sequences were as follows: TBP (forward 5′-CACGAACCACGGCACTGATT-3′; reverse 5′-TTTTCTGCTGCC-AGTCTGGAC-3′; probe 5′-FAM-TCTTCACTCTTGGCTCCTGTG-CACA-TAMRA-3′), HPRT1 (forward 5′-GCTTTCCTTGGTCAGG-CAGTA-3′; reverse 5′-GTCTGGCTTATATCCAACACTTCGT-3′; probe, 5′-FAM-TCAAGGTCGCAAGCTTGCTGGTGAAAAGGA-TAMRA-3′), *KLK3* (forward 5′-GTCTGCGGCGGTGTTCTG-3′; reverse 5′-TGCCGACCCAGCAAGATC-3′; probe 5′-FAM-CACAG-CTGCCCACTGCATCAGGA-TAMRA-3′), *AR* (forward 5′-AGG-ATGCTCTACTTCGCCCC-3′; reverse 5′-ACTGGCTGTACATCC-GGGAC-3′; probe 5′-FAM-TGGTTTTCAATGAGTACCGCA-TGCACA-TAMRA-3′). *NR3C1* (Hs00353740_m1), *SGK1* (Hs00985033_g1), *FKBP5* (Hs01561006_m1) TaqMan gene expression assays (Thermo Fisher Scientific) were used according to the manufacturer's protocol.

Western blot analysis

Western blot analysis was performed as described previously (30). The following antibodies were used: anti-GAPDH (1:50,000; Millipore MAB374), anti-AR (1:500; Santa Cruz Biotechnology sc-816), and anti-GR rabbit mAb (D6H2L; 1:500; Cell Signaling Technology).

Proliferation measurements

Proliferation was assessed using [^{3}H]thymidine incorporation as described previously (30). Viability was measured with WST assay according to the manufacturer's protocol. Briefly, 2,500 (PC3, DU145, CWR22Rv1, LAPC4) or 5,000 (DUCaP) cells per well were seeded and treated twice with the indicated drug within a period of 6 days. Measurements were done in at least three independent biological experiments with at least three technical replicates.

3D-spheroid assay

Spheroid formation was assessed using Perfecta3D 96-well hanging drop plates (Sigma). Cell spheroids were imaged on a JuLI fluorescence microscope (NanoEntek). Spheroid size was

evaluated using the free software ImageJ (NIH, Bethesda, MD). Spheroid size was determined using the formula for the geometric mean radius $= 1/2 \, (a \times b)^{1/2}$, where a and b are the two orthogonal diameters of the spheroid as described in detail elsewhere (31–33).

For single GR knockdown experiments, 7,500 (DU145, PC3, LAPC4, CWR22Rv1) or 8,000 (DUCaP) cells were suspended in a final volume of 40 µL/well in the absence or presence of 1 µg/mL doxycycline and cultured for 8 days. On day 4, 20 µL old medium was replaced by 30 µL of fresh medium containing the appropriate amounts of doxycycline. For single RU-486 treatment experiments, 7,500 (LAPC4, CWR22Rv1) or 8,000 (DUCaP) cells were suspended in a final volume of 40 µL/well in the absence or presence of 6 µmol/L RU-486 (LAPC4) or 12 µmol/L RU-486 (CWR22Rv1, DUCaP) and cultured for 8 days. For combined drug treatment experiments, 7,500 LAPC4, CWR22Rv1, and LNCaPabl-Abi/Enza cells were suspended in a final volume of 40 µL/well in the absence or presence of 2.5 µmol/L abiraterone and/or 6 µmol/L RU-486 (for LAPC4), 12 µmol/L RU-486 (CWR22Rv1), or 12 µmol/L RU-486 (LNCaPabl-Abi/Enza) and cultured for 8 days. For single and combination treatment experiments, 20 µL old medium was replaced by 30 µL of fresh medium containing the appropriate amounts of RU-486 or abiraterone after 4 days.

Flow cytometry

A total of 500,000 DU145shGR-2 or LNCaPabl-Abi cells/time point were stained with either Alexa Fluor 488–conjugated anti-GR (D8H2) XP rabbit mAb (1:50; Cell Signaling Technology), or with Alexa Fluor 488–conjugated rabbit (DA1E) mAb XP isotype control (1:50; Cell Signaling Technology) and incubated according to the manufacturer's protocol. To assess GR expression, the percentage of GR^{low} and GR^{high} cell subpopulation was assessed using a FACSCalibur (Becton Dickinson). Time points chosen were: T0 = passage 62–65 (before abiraterone treatment), T1 = passage 88–91, T2 = passage 111–114, T3 = passage 129–132, and T4 = passage 165–168.

Statistical analysis

SPSS (V24.0) and GraphPad Prism 5 were used for statistical analyses. For all experiments, Gaussian distribution was determined using Kolmogorov–Smirnov and D'Agostino and Pearson omnibus normality test. Differences between treatment groups were analyzed using Student t test or Mann–Whitney U test depending on Gaussian distribution. Comparison of multiple treatment groups was done using one/two-way ANOVA and corrected for multiple testing using Bonferroni or Dunn multiple comparison test method depending on Gaussian distribution. Correlation analysis was performed by the Spearman ρ method. Differences in recurrence-free survival were assessed using Kaplan–Meier plots and log-rank test. P values below 0.05 were considered statistically significant. All differences highlighted by asterisks were statistically significant as encoded in figure legends (*, $P < 0.05$; **, $P < 0.01$; ***, $P < 0.001$). Data are presented as mean + SE unless otherwise specified.

Results

GR expression is reduced in primary prostate cancer, restored in metastases, and correlates with reduced progression-free survival in relapse patients

Expression analysis in cryo-conserved tissue from 40 hormone-naïve prostate cancer patients revealed significantly reduced GR

mRNA levels in tumor tissue when comparing GR expression levels of all tumor tissue specimens versus benign samples (Fig. 1A), but also when analyzing differences in GR mRNA between tumor and corresponding matched benign tissue from each patient individually (Fig. 1B). Consistently, GR protein was also downregulated in the majority of malignant tissue samples from the same patients (Fig. 1C). In concordance, comparison of 413 analyses available in the Oncomine database revealed significantly reduced GR gene expression in the majority of investigated malignancies (Fig. 1D). For prostate cancer, the Varambally-Prostate (34), Wallace-Prostate (35), Arredouani-Prostate (36), and Vanaja-Prostate (37) datasets showed significantly reduced GR gene expression in cancerous tissues (Fig. 1E). Furthermore, qRT-PCR results were confirmed by IHC staining of two independent TMAs (n = 177 patients) using a specific GR antibody (Supplementary Fig. S1A and S1B; Fig. 2A and B). In general, an intense GR staining was observed in benign stromal and basal epithelial cells as well as intermediate staining in luminal cells. In cancer tissue, stromal GR staining remained unchanged while it was reduced in luminal cells. Interestingly, metastatic lesions exhibited intermediate or strong GR staining (Fig. 2C). Statistical analysis revealed significantly reduced GR levels in cancerous tissues of each cohort (Fig. 2D). Moreover, combining both cohorts and inclusion of 14 metastatic lesions confirmed reduced GR expression in primary cancer but GR reexpression in metastatic lesions (Fig. 2E). Subsequent stratification in low Gleason score (GSC; ≤6), intermediate GSC (7), and high GSC (>7) cases did not yield further significant differences (Supplementary Fig. S1C). In addition, we assessed the association of GR expression in tumor tissue with time to relapse. Of 24 patients with confirmed biochemical relapse within 10 years after RPE, those with intermediate-high (IRS ≥ 3.5) GR expression had a significantly shorter time to relapse (median, 13 months) than patients with low (IRS ≤ 3.5) GR expression (median, 43 months; Fig. 2F). In addition, screening of different human prostate cell lines revealed high GR mRNA/protein levels in benign EP156T, RWPE1, and BPH1 cells. AR-positive LNCaP, LNCaPabl, DUCaP, VCaP, LAPC4, and CWR22Rv1 cancer cell lines exhibited only weak GR mRNA/protein expression, whereas it was higher in AR-negative PC3 and DU145 cells (Fig. 3A). Notably, we observed an inverse expression of GR and AR in all tested cell models. This negative relationship was confirmed in patients who exhibited significantly higher AR expression in cancer tissue (Supplementary Fig. S1D). However, patient-matched GR/AR expression analysis in tumor tissue revealed no biologically relevant correlation (Supplementary Fig. S1E).

GR is critical for prostate cancer cell proliferation and 3D-spheroid formation

Altered GR expression can have consequences on cell survival (19). To verify this, we generated PC3, DU145, CWR22Rv1, LAPC4, and DUCaP cell sublines transduced with doxycycline-inducible lentiviral shGR vectors (shGR-1, shGR-2). Doxycycline-induced GR knockdown (Fig. 3B; Supplementary Fig. S2A) resulted in diminished cell proliferation (Fig. 3C; Supplementary Fig. S3C). In addition, in most of the investigated cell models also, elevated apoptosis was observed (Supplementary Fig. S2C). Moreover, PC3, DU145, CWR22Rv1, and LAPC4 cells exhibited an impaired ability to form 3D-spheroids, whereas DUCaP did not form compact spheroids upon GR knockdown at all (Fig. 3D;
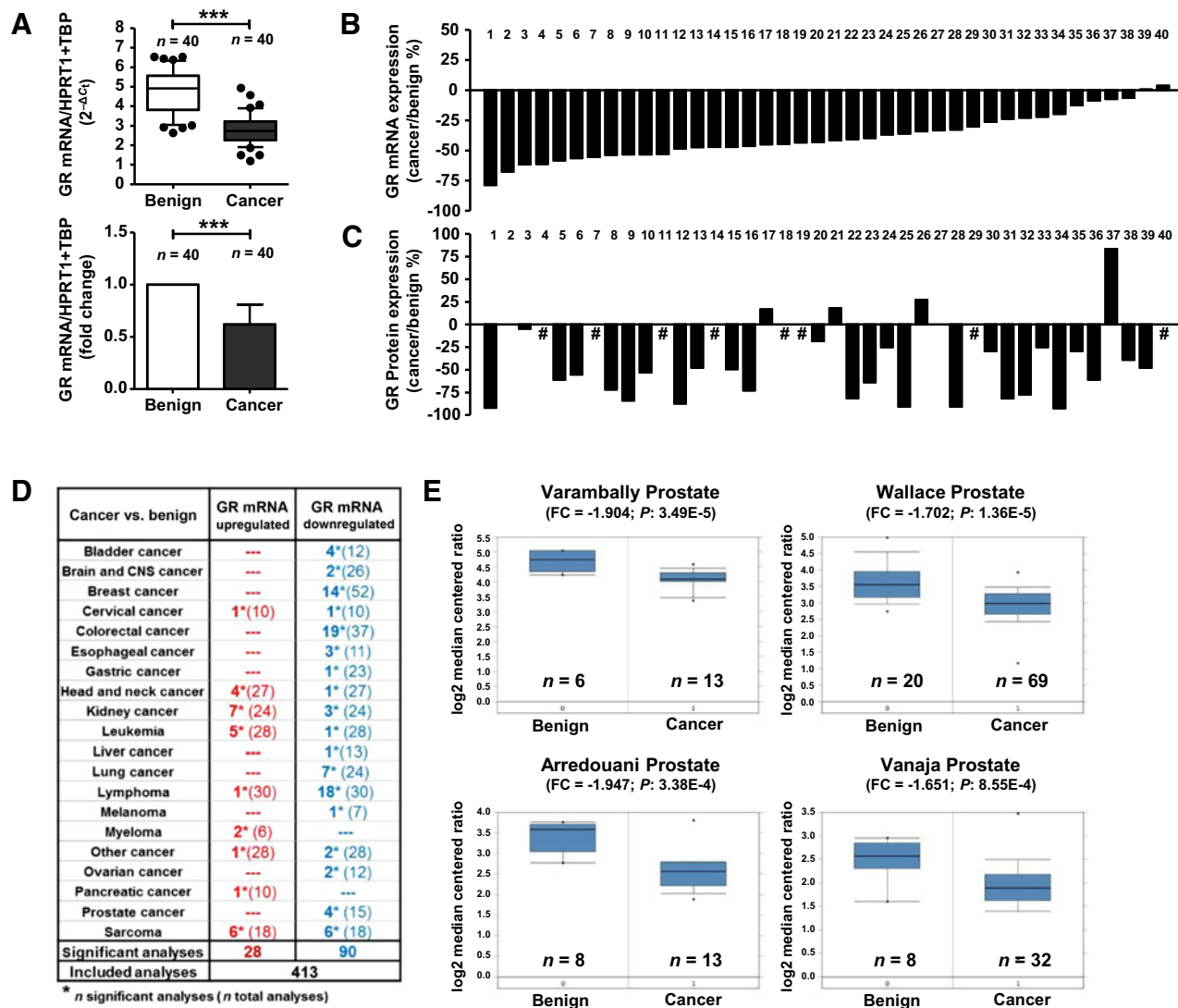
Figure 1.
A, Significantly reduced GR mRNA expression in cancer compared with corresponding benign tissue samples using $2^{-\Delta C_t}$ (top; ***, $P < 0.001$; box whisker plot with 10–90 percentile) or fold change (bottom; data, mean + SD; ***, $P < 0.001$) method. **B** and **C,** Waterfall plot of GR mRNA (**B**) and protein expression (**C**) in tumor tissue, calculated as % of GR expression in benign tissue from each patient (# no protein data available). **D,** Publicly available analyses of GR gene expression in different malignancies in the Oncomine database (threshold P value, 0.01; threshold fold change, 1.5; top 10%, data type all). **E,** Four of 15 analyses revealed significantly reduced GR gene expression in prostate cancer datasets.

Supplementary Fig. S3). Next, we applied the clinically used GR inhibitor RU-486 to block GR-mediated signaling. First, the IC$_{50}$ concentration of RU-486 was determined in LAPC4 (3 μmol/L) and CWR22Rv1 (6 μmol/L) cells (Supplementary Fig. S4A and S4B). RU-486 can also inhibit the progesterone receptor (PR). However, this can be neglected in our experimental setting, given that PR is not expressed in the prostate cancer cell models employed (Supplementary Fig. S5). Similar to GR knockdown above, pharmacologic GR inactivation also decreased cell proliferation, reduced cell number, and diminished 3D-spheroid growth (Fig. 4A and B; Supplementary Fig. S6A). We observed reduced GR and surprisingly reduced AR levels upon GR inhibition (Fig. 4A and B) in LAPC4 and CWR22Rv1, both in 2D (top) and in 3D (bottom) culture conditions. In addition, GR inacti-

vation led to reduced 2D-colony formation with significantly smaller colony size in CWR22Rv1 cells (Supplementary Fig. S6B).

GR inhibition enhances the antitumor effects of abiraterone

As GR signaling has proven to be critical for cancer cell proliferation and seems to influence AR expression, we hypothesized that combined GR inhibition and AR signaling blockade might improve the therapeutic efficacy of abiraterone. It has recently been shown that abiraterone not only blocks CYP17A1, but also can bind to AR. It is additionally converted to Δ4-abiraterone, which acts as an AR antagonist with a potency similar to enzalutamide (38, 39). Abiraterone decreased GR as well as AR levels, albeit only in androgen-dependent LAPC4 and not in androgen-independent CWR22Rv1 cells (Fig. 4C). Surprisingly, GR and AR
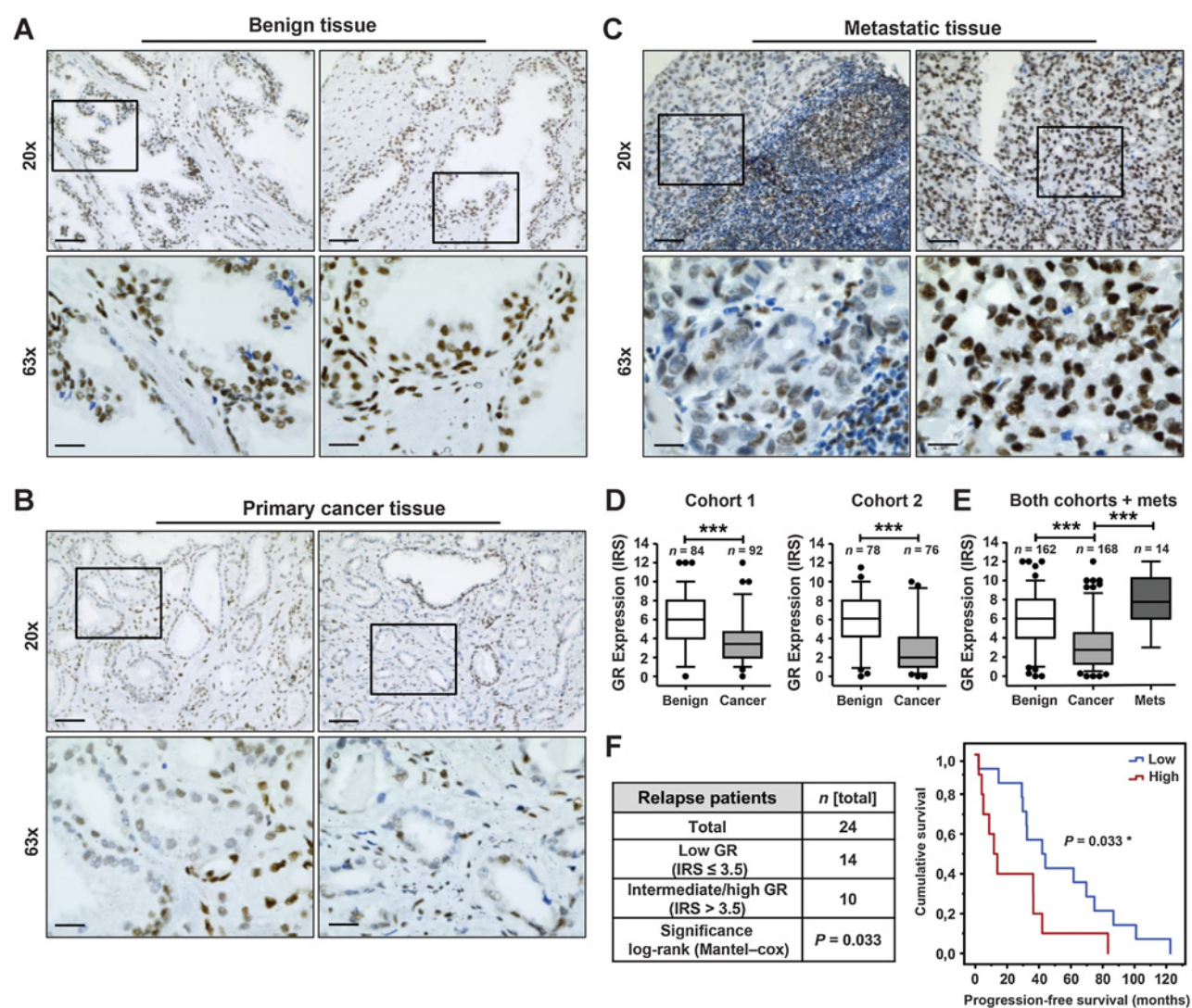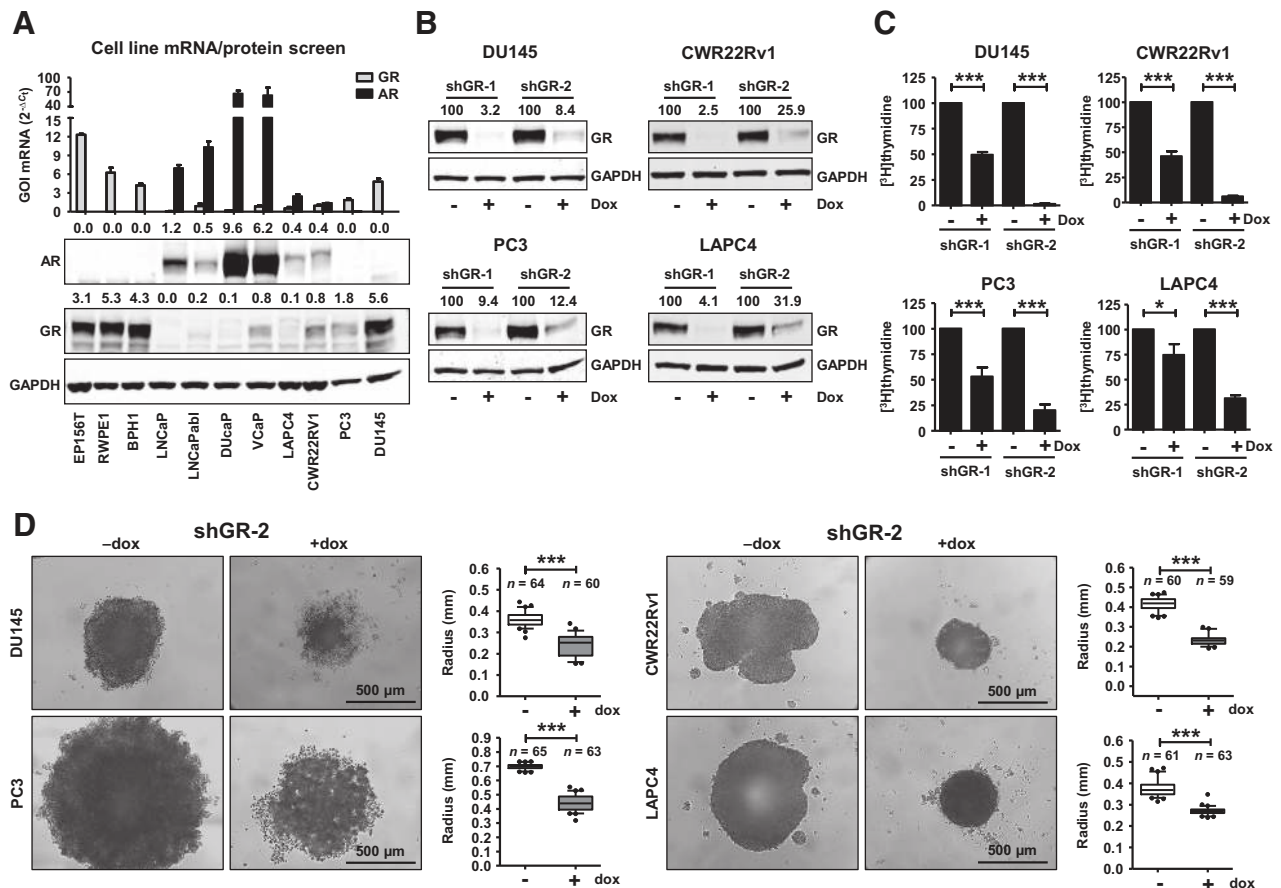
Figure 2.
A–C, Representative microscopy images of benign, primary prostate cancer tissue, and lymph node metastases for GR expression. Magnification, ×20 (scale bar = 50 μm) and ×63 (scale bar = 20 μm). **D,** Quantification of GR immunoreactivity scores (IRS) after IHC staining of two TMAs comprising benign and tumor tissue samples of two independent cohorts (***, $P < 0.001$; box whisker plot with 5–95 percentile). **E,** Quantification of GR IRS after combination of both cohorts and inclusion of tissue from 14 metastatic lesions (***, $P < 0.001$; box whisker plot with 5–95 percentile). **F,** Kaplan–Meier analysis of progression-free survival [progression is defined as rerising PSA levels (>0.2 ng/mL) within at least 2 consecutive measurements] of tumor relapse patients with intermediate/high (IRS ≥ 3.5) or low (IRS ≤ 3.5) GR expression in tumor sections [log-rank (Mantel–Cox); $P = 0.033$].

protein reduction was not accompanied by diminished mRNA expression (Fig. 4D) and is thus not a transcriptional event. Consistent with receptor downregulation, RU-486 as well as abiraterone treatment yielded reduced expression of GR/AR target genes KLK3 and FKBP5 in androgen-dependent LAPC4 but not in androgen-independent CWR22Rv1 (Fig. 4E). Notably, the combined treatment reduced cell number (Supplementary Fig. S6C) and, more importantly, significantly diminished 3D-spheroid growth in both cell lines (Fig. 5A and B).

GR is increased in long-term abiraterone-treated prostate cancer cells

Arora and colleagues reported that elevated GR expression can trigger enzalutamide resistance by bypassing AR blockade

(18). Thus, we aimed to assess whether this might account also for abiraterone insensitivity. To this end, long-term (>10 months) abiraterone-treated LNCaPabl-Abi, LAPC4-Abi, and DUCaP-Abi cells were generated. All established sublines displayed reduced sensitivity to abiraterone (Supplementary Fig. S7A and S7B). In contrast to LAPC4-Abi, GR mRNA/protein was elevated in DUCaP-Abi and LNCaPabl-Abi cells (Supplementary Fig. S8), which could be attributed to a stepwise gain of GR in abiraterone-treated but not in control cells (Fig. 5C; Supplementary Fig. S9A). Flow cytometry confirmed an increasing GR^high cell subpopulation in LNCaPabl-Abi cells over time (Fig. 5D; Supplementary Fig. S9B and S9C). Importantly, abiraterone withdrawal for 5 weeks did not result in a significant reversal of GR mRNA/protein expression (Fig. 5E). Thus, we

Figure 3.
A, mRNA and protein screen for GR and AR expression in benign (EP156T, RWPE1, and BPH1), cancerous AR-positive (LNCaP, LNCaPabl, DUCaP, VCaP, LAPC4, and CWR22Rv1) as well as in cancerous AR-negative (PC3 and DU145) cells was performed by qRT-PCR and Western blot analysis, respectively.
B, GR knockdown confirmation by Western blot analysis using two specific doxycycline-inducible shGR-RNA sequences (shGR-1 and shGR-2) after activation with 1 μg/mL doxycycline for 6 days in DU145 and PC3. **C,** Cell proliferation ([³H]thymidine incorporation) measurement after activation of shGR-1 and shGR-2 with 1 μg/mL doxycycline for 6 days (data, mean + SE from at least three independent experiments; ***, P < 0.001). **D,** 3D spheroid formation after GR knockdown in DU145, PC3, CWR22Rv1, and LAPC4 cells with 1 μg/mL doxycycline for 8 days (box whisker plots with 10–90 percentile represent data from three independent experiments; ***, P < 0.001).

conclude that increased GR levels arise via a stable clonal selection.

### Elevated GR is a general consequence of antiandrogen treatment

We next aimed to assess whether observed changes are limited to abiraterone or represent a general mechanism of cancer cell survival during long-term antiandrogen treatment also with other drugs. We therefore analyzed previously described long-term enzalutamide (LNCaPabl-Enza, LAPC4-Enza, and DUCaP-Enza; (8)) as well as newly generated LNCaP-Enza cells. Importantly, all but one long-term enzalutamide-treated cell sublines displayed significantly increased GR mRNA/protein expression (Supplementary Fig. S10). It thus can be concluded that GR induction is a frequent survival mechanism for prostate cancer cells under endocrine therapy, considering that 5 of 7 long-term antiandrogen-treated cell lines overexpress GR.

For further experiments, we chose LNCaPabl-Abi (abl-Abi) and LNCaPabl-Enza (abl-Enza) as the most representative cell models

for abiraterone- and enzalutamide-insensitive mCRPC and directly compared GR mRNA/protein levels (Fig. 6A). Notably, the highly expressed GR is functionally active, as determined by expression of serum glucocorticoid kinase 1 (SGK1), a well-known and direct GR target gene. Dexamethasone-induced SGK1 expression was significantly higher in both cell sublines compared with vehicle (EtOH)-treated cells (Fig. 6B). To verify that GR and not AR is the crucial transcription factor that induces SGK1, we blocked either GR (siGR + RU-486) or AR (siAR + enzalutamide; Supplementary Fig. S11A). Although AR blockade did not change dexamethasone-induced SGK1 expression, GR blockade significantly decreased SGK1, demonstrating that elevated SGK1 is solely a consequence of GR activation in these cells (Fig. 6C).

GR targeting is effective in long-term antiandrogen-treated prostate cancer cells

To further evaluate the potential use of GR inhibition for antiandrogen-insensitive cells, we performed single and combination treatments with RU-486 and abiraterone in abl-Abi and
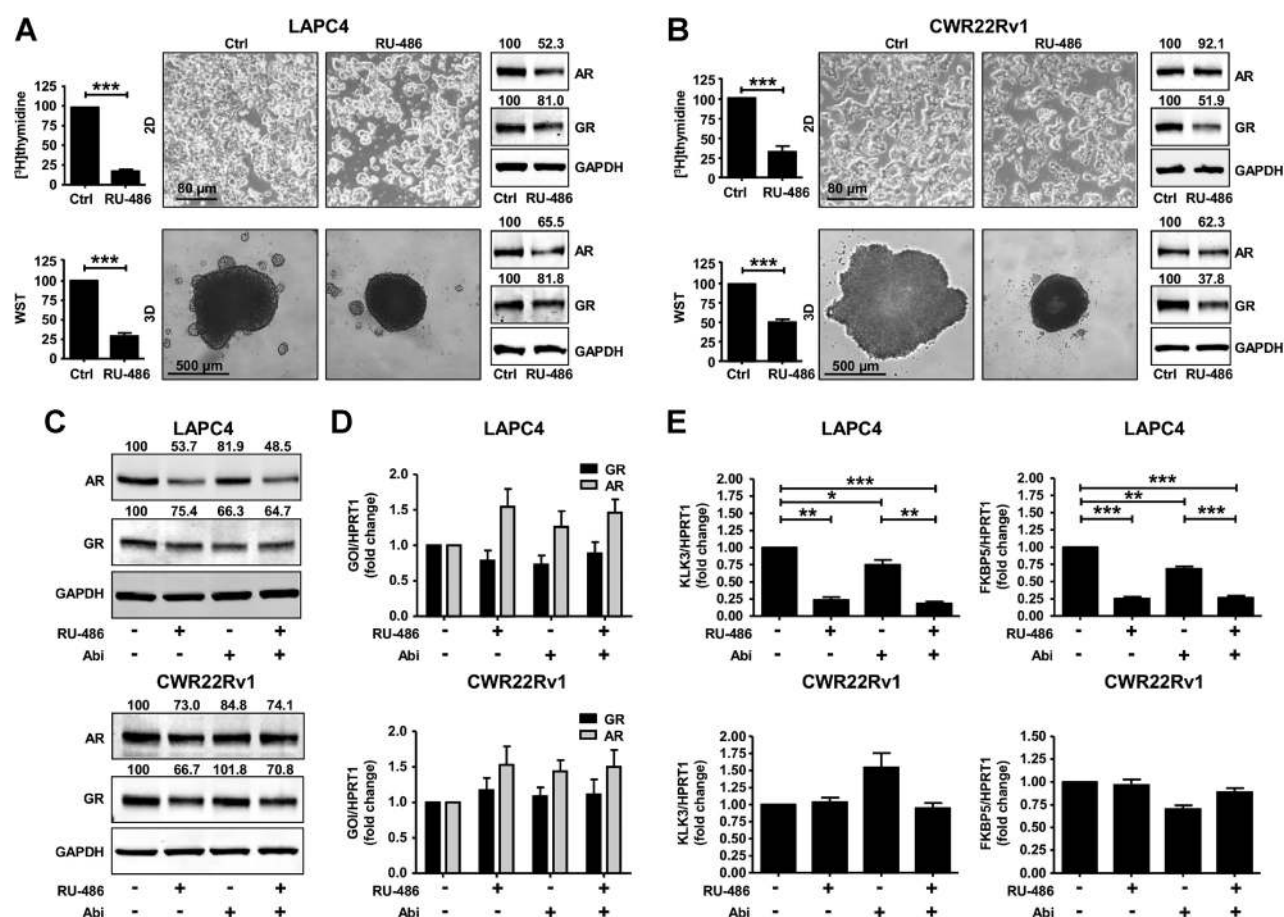
Figure 4.
A and **B,** Cell proliferation and microscopy images in 2D/3D conditions as well as representative Western blots after 6-day RU-486 treatment in LAPC4 (**A**; 3 μmol/L RU-486) and CWR22Rv1 (**B**; 6 μmol/L RU-486) cells. Proliferation was determined by [³H]thymidine incorporation (top) and WST assay (bottom). Data, mean + SE from at least three independent experiments; ***, P < 0.001. **C–E,** GR/AR protein (**C**) and mRNA screen (**D**) in LAPC4 and CWR22Rv1 cells after single/combination treatment as well as evaluation of GR/AR downstream genes KLK3 and FKBP (**E**) after RU-486 and abiraterone treatment (3 μmol/L RU-486, 2.5 μmol/L abiraterone for LAPC4; 6 μmol/L RU-486, 2.5 μmol/L abiraterone for CWR22Rv1) for 6 days [data, mean + SE from at least three independent experiments (*, P < 0.05; **, P < 0.01; ***, P < 0.001)].

abl-Enza cells. As expected, abiraterone treatment had no significant impact on cell proliferation in abl-Abi cells, while it reduced proliferation in abl-Enza cells by approximately 40% (Fig. 6D). Importantly, however, RU-486 alone resulted in a massive decrease in cell proliferation (∼70%; Fig. 6D), reduced cell number and viability (Supplementary Fig. S11B and S11C), and impaired 3D-spheroid formation in both cell models (Fig. 6E). Moreover, combined treatment was superior to abiraterone single treatment in abl-Abi and abl-Enza cells.

Discussion

In this study, we show that GR expression is significantly decreased in primary prostate cancer tissue. This finding might be explained by the fact that GR levels can be negatively regulated by AR signaling (20), which is highly active in primary as well as castration-resistant prostate cancer. Supportively, we detected high GR expression in benign or malignant cell lines with low or absent AR expression, whereas in malignant AR-positive cell lines, GR levels were decreased. Furthermore, we found a general inverse GR/AR expression in prostate tissue samples, although patient-matched analysis did not reveal a biologically relevant correlation (40). It should be noted that AR expression does not necessarily reflect the transcriptional activity of the receptor within the cells. Notably, although expressed at lower levels, GR was present in 165 of 168 analyzed tumors. Moreover, our *in vitro* experiments demonstrate that GR is crucial for cancer cell proliferation, regardless of whether GR levels were high or low. Importantly, we detected restoration of GR expression in hormone therapy–naïve lymph node metastases removed at the time of RPE. The mechanistic background of GR restoration in metastases is currently not known. Interestingly, it has been demonstrated that the transcription factor Yin Yang 1 is able to upregulate GR in hepatic cells (41). Yin Yang 1 supports proliferation, EMT, and metastases (42) and has been frequently found upregulated in prostate cancer (43). Thus, it is possible that Yin Yang 1 contributes to GR restoration in metastases even in hormone-naïve stages. On the basis of our results, it is conceivable that GR blockade might be a therapeutic option already in hormone therapy–naïve tumor stages.
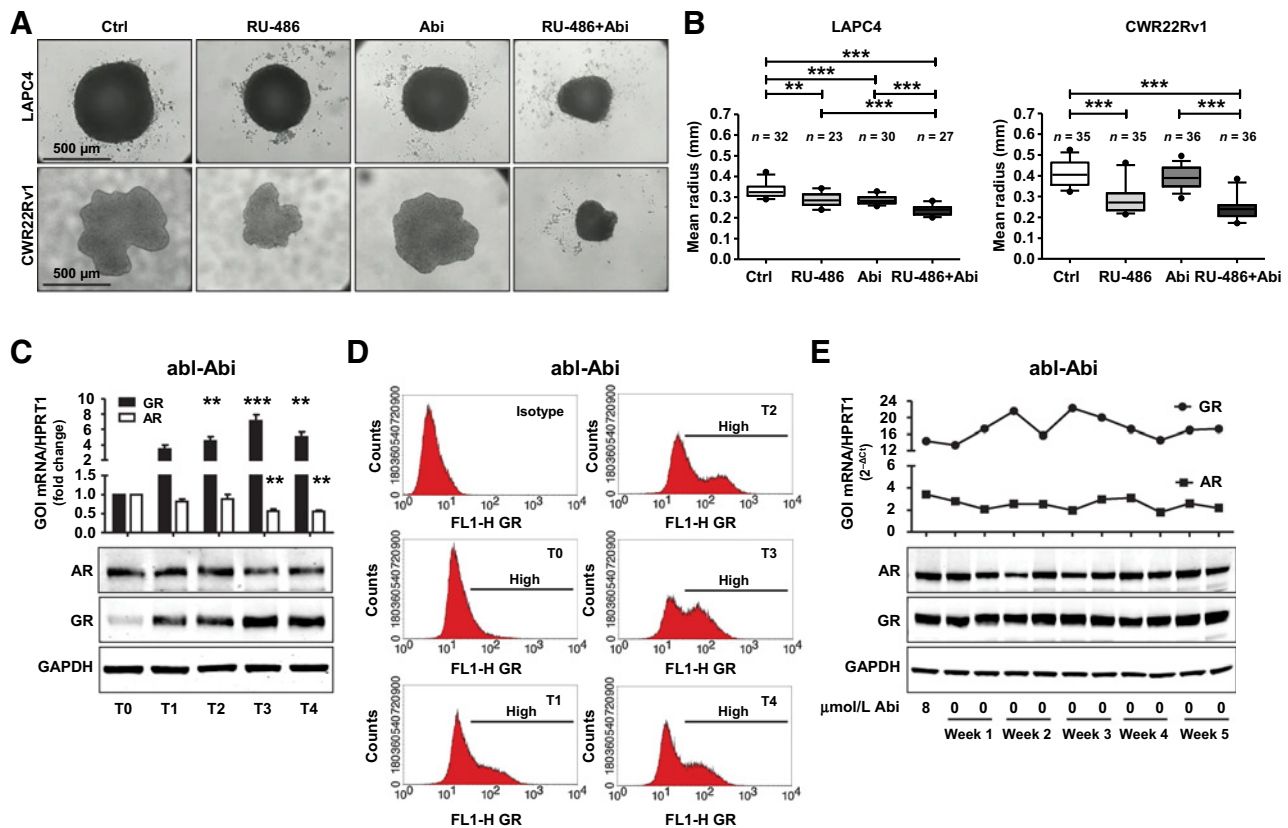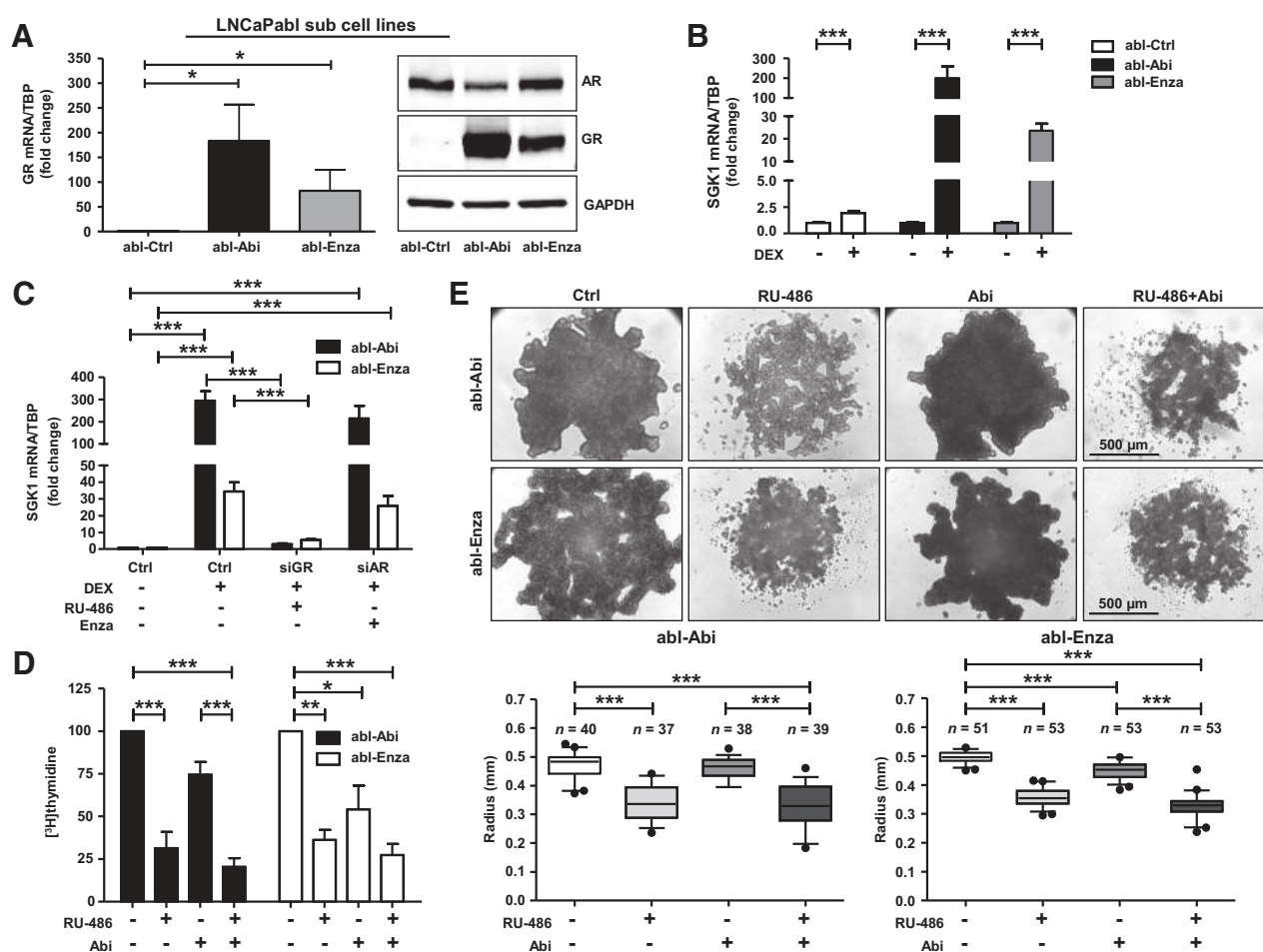
Figure 5.
A and **B,** Representative images (**A**) and quantification (**B**) of LAPC4 and CWR22Rv1 3D-spheroids after 8 days of single/combined treatment with RU-486 and abiraterone (6 μmol/L RU-486, 2.5 μmol/L abiraterone for LAPC4; 12 μmol/L RU-486, 2.5 μmol/L abiraterone for CWR22Rv1). Data, mean + SE from at least three independent experiments (***, $P < 0.001$). **C** and **D,** Determination of a step-wise increase of GR expression in different passages of long-term abiraterone-treated LNCaPabl-Abi (abl-Abi) cells before and during 1 year of cultivation with abiraterone by qRT-PCR and Western blot [**C;** data represent mean + SE from 4 consecutive passages of each time point (*, $P < 0.05$; **, $P < 0.01$; ***, $P < 0.001$)] or flow cytometry analysis (**D**). **E,** qRT-PCR and Western blot analysis of GR mRNA and protein following abiraterone withdrawal in LNCaPabl-Abi for 5 weeks.

In a previous study, we linked GR expression and therapy resistance, showing that GR is elevated in docetaxel-resistant cell lines as well as in patients after chemotherapy (23). Moreover, it has been demonstrated that GR is elevated in bone metastases of prostate cancer patients following enzalutamide therapy and that high GR levels correlate with poor prognosis. The same study showed that GR is upregulated in LNCaP/AR xenografts and cell lines that resume growth in the presence of enzalutamide or ARN-509 and that GR can partly drive expression of AR target genes in these models (18). Consistently, a recent publication suggested that this GR takeover is mediated by loss of cortisol-inactivating enzyme 11β-HSD2, leading to sustained cortisol concentrations in enzalutamide-resistant tumor cells (44). These reports indicate a considerable role of GR in therapy resistance not only to docetaxel but also to antiandrogens. In the current study, we confirmed and further extended these findings by assessing GR expression in multiple long-term abiraterone- and enzalutamide-treated cells generated from parental prostate cancer cell lines of different metastatic origin. We revealed that GR is increased in 5 of 7 long-term antiandrogen-treated cell lines. The only models that do not exhibit an increase in GR expression compared with controls are LAPC4-Abi/Enza cell sublines. This mechanistic

difference might be explained by the fact that, unlike the other cell models employed, LAPC4 are cultured in the permanent presence of DHT, which might compete with the antiandrogens used. Moreover, in LAPC4-Enza cells, enzalutamide resistance is most likely driven by AR amplification as well as gain of AR-V7 expression (8, 45). Despite this exception, GR upregulation seems to be a very frequent response to long-term antiandrogen treatment. This was furthermore confirmed by Xie and colleagues who reported increased GR expression in prostate cancer tissue during neoadjuvant hormone therapy (20). Collectively, these findings suggest that GR overexpression is not a rare, cell line or drug-specific phenomenon but, rather a general mechanism, allowing prostate cancer cells to overcome growth inhibition by multiple drugs that target AR signaling. Mechanistically, the increase in GR expression upon antiandrogen treatment might be a direct consequence of AR inhibition, given that AR has been identified as direct negative regulator of GR expression (20).

To assess effects of GR blockade, we employed shGR knockdown or pharmacologic GR inhibition with RU-486. Notably, either GR knockdown or chemical inhibition alone reduced proliferation and 3D-colony formation in androgen-independent (PC3, DU145) and hormone therapy–naïve (CWR22Rv1, LAPC4,

Figure 6.
A, Elevated GR mRNA and protein expression in LNCaPabl-Abi (abl-Abi) and LNCaPabl-Enza (abl-Enza) compared with LNCaPabl-Ctrl (abl-Ctrl) cells [data represent mean + SE from at least three independent experiments (*, $P < 0.05$)]. **B,** Elevated GR is functional in abl-Abi and abl-Enza sublines, as shown by qRT-PCR analysis of the GR target gene SGK1 after treatment with 1 μmol/L dexamethasone (DEX) for 8 hours [data represent mean + SE from at least three independent experiments (***, $P < 0.001$)]. **C,** Dexamethasone induced SGK1 expression in abl sublines after inhibition of GR or AR expression and activity using 40 nmol/L siGR/AR for 2 days and 12 μmol/L RU-486/4 μmol/L enzalutamide for 1 day prior to 8-hour dexamethasone (1 μmol/L) treatment [data represent mean + SE from at least three independent experiments (***, $P < 0.001$)]. **D,** Proliferation of abl-Abi and abl-Enza cells was measured by [³H]thymidine incorporation upon treatment with 12 μmol/L RU-486 and/or 8 μmol/L abiraterone for 6 days [data represent mean + SE from at least three independent experiments (*, $P < 0.05$; ***, $P < 0.001$)]. **E,** Representative images and statistical analysis of 3D-spheroid formation of abl-Abi and abl-Enza cells after single or combined treatment with 12 μmol/L RU-486 and 8 μmol/L abiraterone for 8 days.

and DUCaP) cells, although DUCaP were less sensitive to GR blockade. This finding may be explained by the fact that these cells exhibit very high AR expression due to gene amplification (8) and consequently decreased GR dependency. Importantly, however, GR blockade as single treatment was highly efficient also in long-term antiandrogen-treated (LNCaPabl-Abi/Enza) cell models. Moreover, in the latter model, a combination of RU-486 and abiraterone was even more effective than abiraterone single treatment. The finding that long-term antiandrogen treatment increases GR expression may also have therapeutic implications. Currently, glucocorticoids are given in combination with different drugs like docetaxel (13, 14), cabazitaxel (15), or abiraterone (16, 17), mainly to ameliorate therapy-related side effects. Albeit beneficial, it should be considered that in such a therapeutic setting, glucocorticoids might further promote selection and

stimulation of GR^high drug-insensitive prostate cancer cells, enhance cell survival, and consequently lead to accelerated disease progression. Considering present and previous results, the exact benefit of glucocorticoids in combination with abiraterone or docetaxel should be carefully reevaluated. For GR inhibition, we used shRNA-mediated knockdown or the competitive GR antagonist RU-486, which has already been tested in clinical trials (NCT00140478, no results published so far; ref. 46) and is currently under investigation in combination with enzalutamide (NCT02012296). However, RU-486 is also known to influence the activity of the PR (47). Importantly, we excluded that any effects are mediated through PR because all used cell lines are negative for this receptor. This is in line with a recent study showing that PR is solely expressed in the benign stromal compartment of the prostate and further decreases in cancer-

associated stroma (48). However, considering PR expression in multiple tissue types of the human body (49), there will be a need for novel GR-specific inhibitors. A promising approach in this respect represents minor groove DNA-binding small molecules targeting nuclear receptor DNA-binding sites. As recently demonstrated in enzalutamide-resistant cells, a pyrrole-imidazole polyamide, targeting the AR/GR consensus site can inhibit both AR and GR signaling as well as transcription (50). As GR determines resistance to antiandrogens, dual AR/GR blockage may be a particularly promising treatment strategy for advanced prostate cancer.

Taken together, the data presented herein provide strong support for the use of GR antagonists for the treatment of endocrine therapy–naïve and resistant prostate cancer. However, it has to be anticipated that systemic administration of a GR inhibitor, even if it binds GR exclusively, might cause multiple adverse effects due to ubiquitous GR expression in virtually all tissue types (11). Further studies are therefore warranted to investigate tumor-specific GR antagonism to potentially avoid systemic effects.

Disclosure of Potential Conflicts of Interest

I. Heidegger reports receiving speakers bureau honoraria from Janssen, is a consultant/advisory board member for, and reports receiving commercial research grants from Bayer. Z. Culig is a consultant/advisory board member for and reports receiving commercial research grants from Astellas. H. Klocker is a consultant/advisory board member for Astellas. No potential conflicts of interest were disclosed by the other authors.

Authors' Contributions

Conception and design: M. Puhr, I. Heidegger, G. Van der Pluijm
Development of methodology: M. Puhr, G. Schaefer, I. Eder
Acquisition of data (provided animals, acquired and managed patients, provided facilities, etc.): M. Puhr, J. Hoefer, A. Eigentler, C. Ploner, F. Handle, G. Schaefer, J. Kroon, I. Heidegger, H. Klocker
Analysis and interpretation of data (e.g., statistical analysis, biostatistics, computational analysis): M. Puhr, F. Handle, G. Schaefer
Writing, review, and/or revision of the manuscript: M. Puhr, J. Hoefer, A. Eigentler, F. Handle, G. Schaefer, I. Heidegger, I. Eder, Z. Culig, G. Van der Pluijm, H. Klocker
Administrative, technical, or material support (i.e., reporting or organizing data, constructing databases): M. Puhr, A. Eigentler, C. Ploner, G. Schaefer, I. Eder, H. Klocker
Study supervision: M. Puhr, Z. Culig
Other (performed Western blot assays): A. Leo

References

1. Ryan CJ, Smith MR, de Bono JS, Molina A, Logothetis CJ, de Souza P, et al. Abiraterone in metastatic prostate cancer without previous chemotherapy. N Engl J Med 2013;368:138–48.
2. de Bono JS, Logothetis CJ, Molina A, Fizazi K, North S, Chu L, et al. Abiraterone and increased survival in metastatic prostate cancer. N Engl J Med 2011;364:1995–2005.
3. Scher HI, Fizazi K, Saad F, Taplin ME, Sternberg CN, Miller K, et al. Increased survival with enzalutamide in prostate cancer after chemotherapy. N Engl J Med 2012;367:1187–97.
4. Beer TM, Armstrong AJ, Rathkopf DE, Loriot Y, Sternberg CN, Higano CS, et al. Enzalutamide in metastatic prostate cancer before chemotherapy. N Engl J Med 2014;371:424–33.
5. Hu R, Lu C, Mostaghel EA, Yegnasubramanian S, Gurel M, Tannahill C, et al. Distinct transcriptional programs mediated by the ligand-dependent full-length androgen receptor and its splice variants in castration-resistant prostate cancer. Cancer Res 2012;72:3457–62.
6. Li Y, Chan SC, Brand LJ, Hwang TH, Silverstein KA, Dehm SM. Androgen receptor splice variants mediate enzalutamide resistance in castration-resistant prostate cancer cell lines. Cancer Res 2013;73:483–9.
7. Geney R, Ungureanu M, Li D, Ojima I. Overcoming multidrug resistance in taxane chemotherapy. Clin Chem Lab Med 2002;40:918–25.
8. Hoefer J, Akbor M, Handle F, Ofer P, Puhr M, Parson W, et al. Critical role of androgen receptor level in prostate cancer cell resistance to new generation antiandrogen enzalutamide. Oncotarget 2016;7:59781–94.
9. Korpal M, Korn JM, Gao X, Rakiec DP, Ruddy DA, Doshi S, et al. An F876L mutation in androgen receptor confers genetic and phenotypic resistance to MDV3100 (enzalutamide). Cancer Discov 2013;3:1030–43.
10. Kassi E, Moutsatsou P. Glucocorticoid receptor signaling and prostate cancer. Cancer Lett 2011;302:1–10.
11. Oakley RH, Cidlowski JA. The biology of the glucocorticoid receptor: new signaling mechanisms in health and disease. J Allergy Clin Immunol 2013;132:1033–44.
12. Ndibe C, Wang CG, Sonpavde G. Corticosteroids in the management of prostate cancer: a critical review. Curr Treat Options Oncol 2015;16:6.
13. Tannock IF, de Wit R, Berry WR, Horti J, Pluzanska A, Chi KN, et al. Docetaxel plus prednisone or mitoxantrone plus prednisone for advanced prostate cancer. N Engl J Med 2004;351:1502–12.
14. Petrylak DP, Tangen CM, Hussain MH, Lara PN Jr, Jones JA, Taplin ME, et al. Docetaxel and estramustine compared with mitoxantrone and prednisone for advanced refractory prostate cancer. N Engl J Med 2004;351:1513–20.
15. Heidenreich A, Bracarda S, Mason M, Ozen H, Sengelov L, Van Oort I, et al. Safety of cabazitaxel in senior adults with metastatic castration-resistant prostate cancer: results of the European compassionate-use programme. Eur J Cancer 2014;50:1090–9.
16. Small EJ, Lance RS, Gardner TA, Karsh LI, Fong L, McCoy C, et al. A randomized phase II trial of sipuleucel-T with concurrent versus sequential abiraterone acetate plus prednisone in metastatic castration-resistant prostate cancer. Clin Cancer Res 2015;21:3862–9.
17. Kluetz PG, Ning YM, Maher VE, Zhang L, Tang S, Ghosh D, et al. Abiraterone acetate in combination with prednisone for the treatment of patients with metastatic castration-resistant prostate cancer: U.S. Food and Drug Administration drug approval summary. Clin Cancer Res 2013;19:6650–6.
18. Arora VK, Schenkein E, Murali R, Subudhi SK, Wongvipat J, Balbas MD, et al. Glucocorticoid receptor confers resistance to antiandrogens by bypassing androgen receptor blockade. Cell 2013;155:1309–22.
19. Isikbay M, Otto K, Kregel S, Kach J, Cai Y, Vander Griend DJ, et al. Glucocorticoid receptor activity contributes to resistance to androgen-targeted therapy in prostate cancer. Hormones Cancer 2014;5:72–89.
20. Xie N, Cheng H, Lin D, Liu L, Yang O, Jia L, et al. The expression of glucocorticoid receptor is negatively regulated by active androgen receptor signaling in prostate tumors. Int J Cancer 2015;136:E27–38.
21. Lempiainen JK, Niskanen EA, Vuoti KM, Lampinen RE, Goos H, Varjosalo M, et al. Agonist-specific protein interactomes of glucocorticoid and androgen receptor as revealed by proximity mapping. Mol Cell Proteomics 2017;16:1462–74.
22. Zhang C, Wenger T, Mattern J, Ilea S, Frey C, Gutwein P, et al. Clinical and mechanistic aspects of glucocorticoid-induced chemotherapy resistance in the majority of solid tumors. Cancer Biol Ther 2007;6:278–87.

23. Kroon J, Puhr M, Buijs JT, van der Horst G, Hemmer DM, Marijt KA, et al. Glucocorticoid receptor antagonism reverts docetaxel resistance in human prostate cancer. Endocr Relat Cancer 2016;23:35–45.

24. Culig Z, Hoffmann J, Erdel M, Eder IE, Hobisch A, Hittmair A, et al. Switch from antagonist to agonist of the androgen receptor bicalutamide is associated with prostate tumour progression in a new model system. Br J Cancer 1999;81:242–51.

25. Bello D, Webber MM, Kleinman HK, Wartinger DD, Rhim JS. Androgen responsive adult human prostatic epithelial cell lines immortalized by human papillomavirus 18. Carcinogenesis 1997;18:1215–23.

26. Kogan I, Goldfinger N, Milyavsky M, Cohen M, Shats I, Dobler G, et al. hTERT-immortalized prostate epithelial and stromal-derived cells: an authentic in vitro model for differentiation and carcinogenesis. Cancer Res 2006;66:3531–40.

27. Madar S, Brosh R, Buganim Y, Ezra O, Goldstein I, Solomon H, et al. Modulated expression of WFDC1 during carcinogenesis and cellular senescence. Carcinogenesis 2009;30:20–7.

28. Sigl R, Ploner C, Shivalingaiah G, Kofler R, Geley S. Development of a multipurpose GATEWAY-based lentiviral tetracycline-regulated conditional RNAi system (GLTR). PLoS One 2014;9:e97764.

29. Puhr M, Hoefer J, Neuwirt H, Eder IE, Kern J, Schafer G, et al. PIAS1 is a crucial factor for prostate cancer cell survival and a valid target in docetaxel resistant cells. Oncotarget 2014;5:12043–56.

30. Puhr M, Santer FR, Neuwirt H, Susani M, Nemeth JA, Hobisch A, et al. Down-regulation of suppressor of cytokine signaling-3 causes prostate cancer cell death through activation of the extrinsic and intrinsic apoptosis pathways. Cancer Res 2009;69:7375–84.

31. Eder T, Weber A, Neuwirt H, Grunbacher G, Ploner C, Klocker H, et al. Cancer-associated fibroblasts modify the response of prostate cancer cells to androgen and anti-androgens in three-dimensional spheroid culture. Int J Mol Sci 2016;17:pii:E1458.

32. Zhou Y, Arai T, Horiguchi Y, Ino K, Matsue T, Shiku H. Multiparameter analyses of three-dimensionally cultured tumor spheroids based on respiratory activity and comprehensive gene expression profiles. Anal Biochem 2013;439:187–93.

33. Kelm JM, Timmins NE, Brown CJ, Fussenegger M, Nielsen LK. Method for generation of homogeneous multicellular tumor spheroids applicable to a wide variety of cell types. Biotechnol Bioeng 2003;83:173–80.

34. Varambally S, Yu J, Laxman B, Rhodes DR, Mehra R, Tomlins SA, et al. Integrative genomic and proteomic analysis of prostate cancer reveals signatures of metastatic progression. Cancer Cell 2005;8:393–406.

35. Wallace TA, Prueitt RL, Yi M, Howe TM, Gillespie JW, Yfantis HG, et al. Tumor immunobiological differences in prostate cancer between African-American and European-American men. Cancer Res 2008;68:927–36.

36. Arredouani MS, Lu B, Bhasin M, Eljanne M, Yue W, Mosquera JM, et al. Identification of the transcription factor single-minded homologue 2 as a potential biomarker and immunotherapy target in prostate cancer. Clin Cancer Res 2009;15:5794–802.

37. Vanaja DK, Cheville JC, Iturria SJ, Young CY. Transcriptional silencing of zinc finger protein 185 identified by expression profiling is associated with prostate cancer progression. Cancer Res 2003;63:3877–82.

38. Richards J, Lim AC, Hay CW, Taylor AE, Wingate A, Nowakowska K, et al. Interactions of abiraterone, eplerenone, and prednisolone with wild-type and mutant androgen receptor: a rationale for increasing abiraterone exposure or combining with MDV3100. Cancer Res 2012;72:2176–82.

39. Li Z, Bishop AC, Alyamani M, Garcia JA, Dreicer R, Bunch D, et al. Conversion of abiraterone to D4A drives anti-tumour activity in prostate cancer. Nature 2015;523:347–51.

40. Mukaka MM. Statistics corner: A guide to appropriate use of correlation coefficient in medical research. Malawi Med J 2012;24:69–71.

41. Lu Y, Xiong X, Wang X, Zhang Z, Li J, Shi G, et al. Yin Yang 1 promotes hepatic gluconeogenesis through upregulation of glucocorticoid receptor. Diabetes 2013;62:1064–73.

42. Kaufhold S, Garban H, Bonavida B. Yin Yang 1 is associated with cancer stem cell transcription factors (SOX2, OCT4, BMI1) and clinical implication. J Exp Clin Cancer Res 2016;35:84.

43. Seligson D, Horvath S, Huerta-Yepez S, Hanna S, Garban H, Roberts A, et al. Expression of transcription factor Yin Yang 1 in prostate cancer. Int J Oncol 2005;27:131–41.

44. Li J, Alyamani M, Zhang A, Chang KH, Berk M, Li Z, et al. Aberrant corticosteroid metabolism in tumor cells enables GR takeover in enzalutamide resistant prostate cancer. eLife 2017;6:pii:e20183.

45. Antonarakis ES, Lu C, Wang H, Luber B, Nakazawa M, Roeser JC, et al. AR-V7 and resistance to enzalutamide and abiraterone in prostate cancer. N Engl J Med 2014;371:1028–38.

46. Taplin ME, Manola J, Oh WK, Kantoff PW, Bubley GJ, Smith M, et al. A phase II study of mifepristone (RU-486) in castration-resistant prostate cancer, with a correlative assessment of androgen-related hormones. BJU Int 2008;101:1084–9.

47. Benagiano G, Bastianelli C, Farris M. Selective progesterone receptor modulators 1: use during pregnancy. Expert Opin Pharmacother 2008;9:2459–72.

48. Yu Y, Yang O, Fazli L, Rennie PS, Gleave ME, Dong X. Progesterone receptor expression during prostate cancer progression suggests a role of this receptor in stromal cell differentiation. Prostate 2015;75:1043–50.

49. You S, Zuo L, Varma V. Broad tissue expression of membrane progesterone receptor Alpha in normal mice. J Mol Histol 2010;41:101–10.

50. Kurmis AA, Yang F, Welch TR, Nickols NG, Dervan PB. A pyrrole-imidazole polyamide is active against enzalutamide-resistant prostate cancer. Cancer Res 2017;77:2207–12.